J. Phys. Chem. A **2004,** *108,* 403−408

Vibrational Spectra, Ab Initio Calculations, and Conformations of Bicyclo[3.3.0]oct-1,5-ene

Daniel Autrey,[†] Kristjan Haller,[†,‡] Jaan Laane,*[,†] Cornelia Mlynek,[§] and Henning Hopf[§]

Department of Chemistry, Texas A&M University, College Station, Texas 77843-3255, Institute of Physics, University of Tartu, Tartu, 51014 Estonia, and Institut fur Organische Chemie, Technische Universität, Braunschweig, Germany, D-38106 Braunschweig

Received: July 30, 2003; In Final Form: October 17, 2003

The infrared and Raman spectra of bicyclo[3.3.0]oct-1,5-ene in the vapor and liquid phases have been recorded and analyzed. Ab initio calculations, including those with the triple-ζ (cc-pvtz) basis set, have been carried out to predict the energy differences between five different structural forms. Both the spectra and ab initio calculations show that the cis C_{2v} conformation is the lowest energy form. The trans C_{2h} structure is predicted to lie only 65 to 229 cm^{-1} higher in energy, depending on whether the effects of ring flapping are considered, but spectroscopic evidence for this conformation is limited. The dihedral angle of puckering is calculated to be 26°, which is the same as the cyclopentene value.

Introduction

The far-infrared spectra and ring-puckering potential energy function of cyclopentene were first reported by Laane and Lord[1] in 1967. Since then the Raman spectra[2] and vibrational assignments[3] have also been reported as well as refinements of the potential energy function.[4−6] The cyclopentene ring is puckered with a barrier to planarity of 232 cm^{-1} and a dihedral angle of 26°. Although we have examined the potential energy surfaces of numerous cyclic and bicyclic molecules,[7−11] we have never previously examined a bicyclic molecule with two identical rings capable of puckering.

The present paper presents an infrared, Raman, and ab initio study of the bicyclo[3.3.0]oct-1,5-ene molecule (BCO), which can be thought of as two cyclopentene rings joined together and sharing a common double bond. The following paper will present an analysis of the two-dimensional potential energy surface and the associated quantum states for the ring puckering motion. An interesting feature of this molecule is that the two rings are capable of puckering in either the same or opposite directions, resulting in either C_{2v} or C_{2h} symmetry. A planar skeletal structure would have D_{2h} symmetry.

The conformations of this molecule have previously been investigated by electron diffraction,[12] molecular mechanics,[12,13] and "chromatoscopy."[13] Those studies concluded that both rings were puckered and that there are similar amounts of the cis and trans conformations present, resulting from puckering in the same or opposite directions.

Experimental and Computational Methods

The sample of bicyclo[3.3.0]oct-1,5-ene (BCO) was prepared from 1,5-cyclooctadiene (Aldrich, 99%) by C.M. and H.H. in Germany using the method described in the literature.[14] Spectra and gas chromatography showed the product to have greater than 98% purity.

Vapor-phase mid-infrared spectra were recorded on a Bomem DA8.02 Fourier transform interferometer equipped with a DTGS detector. The sample was contained in a 10 cm single pass cell or in a 4.2 or 20 m multipass cell fitted with KBr windows. A germanium-coated KBr beam splitter was used with a glowbar source to record spectra in the 450−7000 cm^{-1} region. Typically 5000−8000 scans at 0.25 cm^{-1} resolution were obtained. Liquid-phase mid-infrared spectra were recorded of a capillary film contained between two polished KBr windows at ambient temperatures on a Biorad FTS-60 Fourier transform interferometer. Typically, 256 scans at 1 cm^{-1} resolution were collected and averaged. Attempts to collect the far-infrared spectra of the sample at room temperature, even at 20 m path length, have proved to be unsuccessful due to the low vapor pressure of the sample and the small dipole moment change associated with the puckering motions.

Raman spectra of the BCO vapor at temperatures between 150 and 180 °C were recorded using an Instruments SA JY−U1000 spectrometer and a Coherent Radiation Innova 20 argon ion laser with excitation at 514.5 nm and 4 W laser power. Both a photomultiplier tube (PMT) and a liquid nitrogen cooled charge-coupled device (CCD) were used as detectors. Spectral resolutions in the 0.5 to 2.0 cm^{-1} range with the PMT and 0.7 cm^{-1} with the CCD were used. The sample was contained in a high-temperature Raman cell previously described.[15] Sample pressures were typically 700 Torr. Liquid-phase Raman spectra were recorded at ambient temperatures. The sample was excited at 532.3 nm using a Coherent DPSS-532 laser operating at 200 mW lasing power. Depolarization measurements were made using a polarizer and scrambler.

Ab initio calculations were carried out using the Gaussian 98 package. Structural parameters and conformational energies were performed at the Møller−Plesset second-order perturbation (MP2) level of theory using the 6-311++G** and triple-ζ (cc-pvtz) basis set. The vibrational frequencies, together with the predicted infrared and Raman intensities, were calculated using the density functional method (B3LYP) and both the 6-31G** and 6-311++G** basis sets.

Computational Results

Relative conformational energies of BCO were calculated using several different basis sets for five different conformations.

---

* Corresponding author.
[†] Texas A&M University.
[‡] University of Tartu.
[§] Technische Universität.

10.1021/jp030940g CCC: $27.50

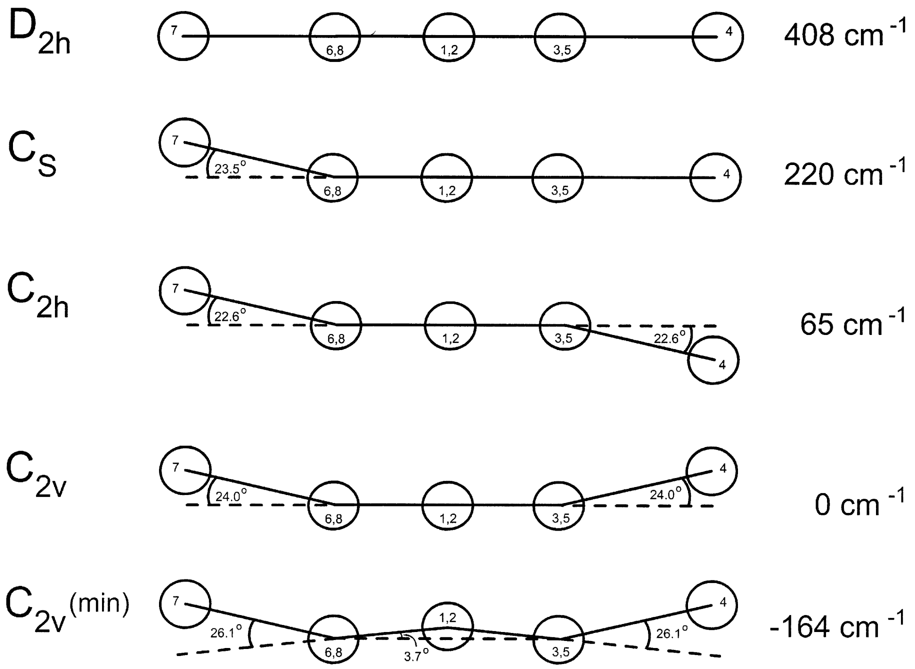

Figure 1. Conformations and calculated relative energies of BCO.

The energy minimum was found to correspond to a W-shaped structure of C_{2v} symmetry where both rings are puckered in the same direction but away from the direction of flapping. This structure along with the computed dihedral angles from the triple-ζ (cc-pvtz) computations is shown in Figure 1. The other four conformations that were considered all assume that the skeletal carbon atoms all lie in the same plane, except for the apex carbons (atoms 4 and 7). The dihedral angles and relative energies were calculated for the planar (D_{2h}), cis (C_{2v}), trans (C_{2h}), and single-ring puckered (C_s) structures, and these are also shown in Figure 1. The energies are expressed relative to the C_{2v} structure (0 cm^{-1}), as this allows the energy difference to be calculated for puckering in the same or opposite directions. The energy minimum is at -164 cm^{-1}, and this shows that the small amount of flapping (3.7° for each ring) reduces the conformational energy by that amount. In the following paper, the theoretical potential energy surface is modeled for the conformers, both with and without flapping. Both the C_{2v} and C_{2h} structures correspond to energy minima with the former being at lower energy (by 229 cm^{-1} for the model where flapping is allowed and by 65 cm^{-1} where there is no flapping). The energy minimum for the trans C_{2h} structure shows no flapping. The relative population of the trans conformation is thus expected to be about 30% of the cis form. The C_s and D_{2h} conformations correspond to a saddle point and energy maximum, respectively, on the potential energy surface, which will be discussed in the following paper. Figure 2 shows the bond lengths and angles from the triple-ζ computation for the C_{2v}, C_{2h}, D_{2h}, and C_s structures. Cyclopentene has a barrier to planarity of 232 cm^{-1} and a dihedral angle of puckering of 26°. To check the reliability of the triple-ζ (cc-pvtz) calculations, we have also carried these out for cyclopentene. These predict a dihedral angle of 26.3° and a barrier of 290 cm^{-1}.

The computed vibrational frequencies using density functional theory (B3LYP) will be compared to the experimental values in the following section. As discussed previously, we have found that we obtain the best comparison between computed and experimental frequencies using the 6-311++G** basis set.[16]

Vibrational Spectra

As discussed above, the BCO molecule typically takes on either C_{2v} or C_{2h} symmetry. However, as will be discussed in the following paper, the ring-puckering motions are large-amplitude and many of the molecules occupy quantum states of the puckering that lie above the barrier to planarity. Hence, D_{2h} selection rules can be used for the most part. Exceptions to these are indicative that the molecule is indeed either C_{2v} or C_{2h}.

In D_{2h} symmetry with the molecule in the *xy* plane, the molecule follows the mutual exclusion rule and has vibrational symmetry species

$$9A_g + 7B_{1g} + 6B_{2g} + 5B_{3g} + 5A_u + 7B_{1u} + 7B_{2u} + 8B_{3u}$$

where the 27 gerade vibrations are Raman active and infrared inactive, while the 22 B_{1u}, B_{2u}, and B_{3u} ungerade vibrations are only infrared active, with vapor-phase band types C, B, and A, respectively. The A_u vibrations are totally inactive. For C_{2v} symmetry the molecule has the vibrational symmetry species

$$16A_1 + 12A_2 + 14B_1 + 12B_2$$

All 54 vibrations are Raman active while the A_1, B_1, and B_2 modes have C, B, and A infrared band types, respectively. For C_{2h} the vibrations have symmetry species

$$15A_g + 12B_g + 12A_u + 15B_u$$

where the 27 gerade vibrations are only Raman active and the 27 ungerade ones are only infrared active. In all symmetries the totally symmetric modes (A_g, A_1, or A_g) are Raman polarized.

Figure 3 shows the vapor-phase infrared and Raman spectra of BCO. Figures 4 and 5 show the liquid-phase infrared and Raman spectra, respectively, compared to the calculated spectra using the 6-311++G** basis set. The calculated frequencies were scaled using a factor of 0.956 for the C$-$H stretching region and 0.981 for frequencies below 1800 cm^{-1}. Figure 5

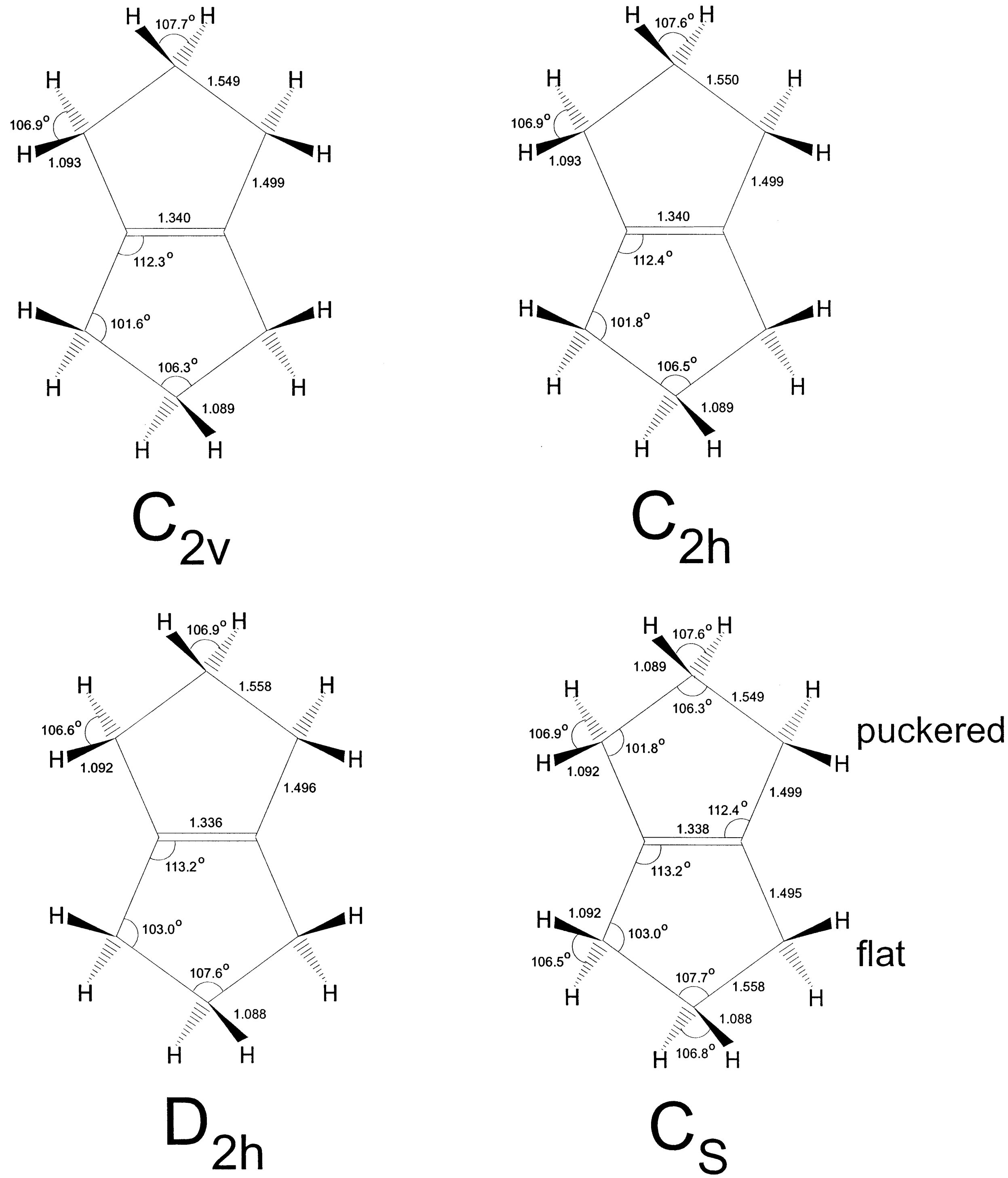

Figure 2. Calculated ab initio structures for BCO for C_{2v}, C_{2h}, D_{2h}, and C_s conformations. The puckering angles are given in Figure 1.

also shows the parallel and perpendicular polarized Raman spectra. Table 1 tabulates both the experimental and calculated frequencies according to D_{2h} symmetry. The corresponding C_{2v} and C_{2h} symmetry species are also indicated as are the selection rules, infrared band types, and Raman polarizations. As can be seen, the D_{2h} selection rules are followed quite well in that the A_g modes all are polarized and are observed in both the vapor-phase and liquid-phase Raman spectra. In addition, the B_{1g}, B_{2g}, and B_{3g} modes are expected to be Raman active and depolarized. Most of these have been observed in the spectra and they are generally depolarized. Bands that are allowed for C_{2v} or C_{2h} symmetry but not D_{2h} are typically weaker if observed at all. In the infrared spectra the B_{1u}, B_{2u}, and B_{3u} modes should be active for D_{2h} symmetry, and most of these bands have been observed in the liquid and/or vapor-phase spectra. The appropriate vapor-phase band types (Q branches for B_{1u} and B_{3u} and type B bands for B_{2u}) were also observed. The primary exceptions to D_{2h} selection rules were the observed polarized Raman bands corresponding to B_{1u} symmetry. Since these are A_1 modes for C_{2v}, this clearly demonstrates the cis puckered conformation is primarily giving rise to those transitions. The depolarized Raman band at 370 cm^{-1} for the liquid corresponding to ν_{46} (skeletal bend) is another confirmation that the C_{2v} structure is present since this vibration is inactive for D_{2h} or C_{2h}. Further evidence that C_{2v} symmetry is dominant comes from the three observed vapor-phase infrared type B bands for

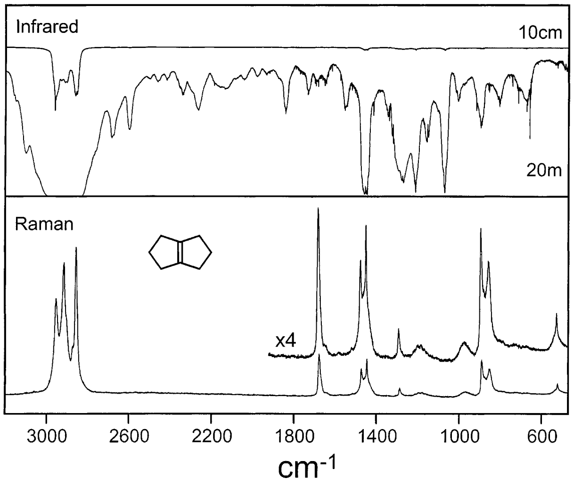

Figure 3. Vapor-phase infrared (1 Torr, 10 cm and 20 m path lengths) and Raman spectra (700 Torr, 170 °C) of BCO.

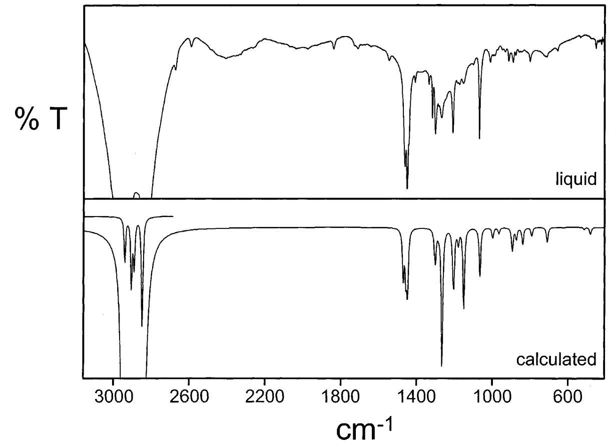

Figure 4. Liquid infrared spectrum of BCO compared to the calculated spectrum (frequencies scaled).

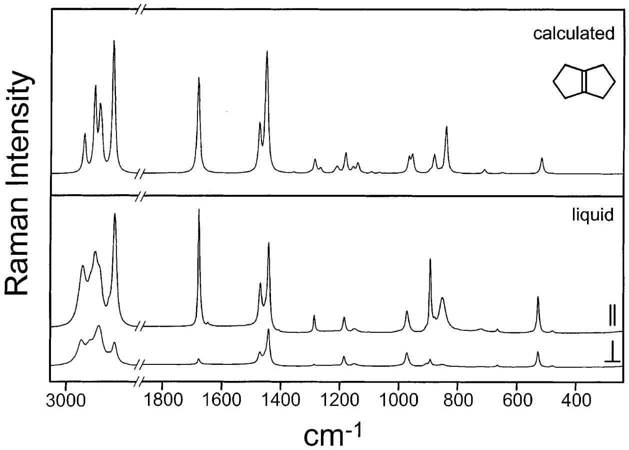

Figure 5. Liquid Raman spectrum of BCO compared to the calculated spectrum (frequencies scaled). The parallel and perpendicular polarized spectra are shown.

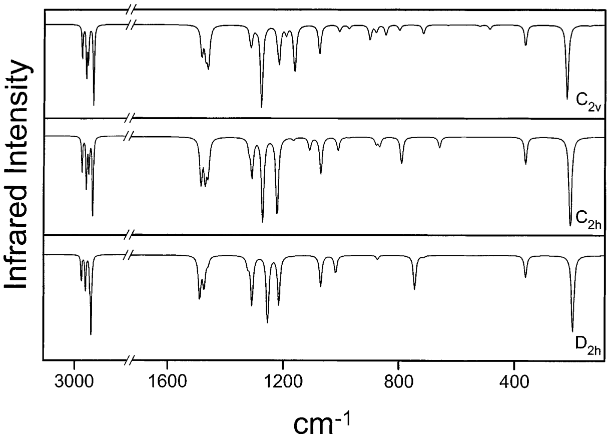

Figure 6. Comparison of the calculated infrared spectra for the D_{2h}, C_{2v}, and C_{2h} structures. The intensities of the CH stretching region have been reduced by 10×.

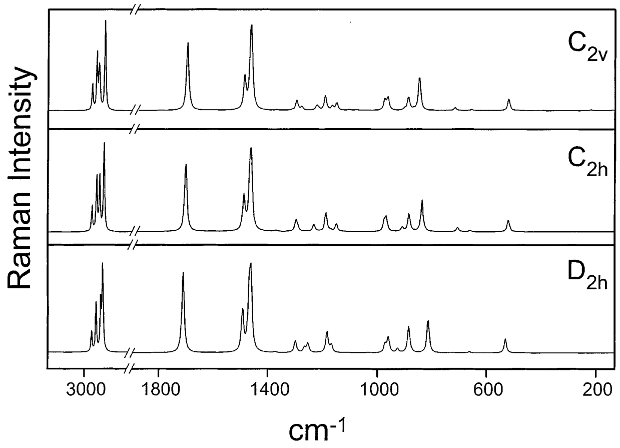

Figure 7. Comparison of the calculated Raman spectra for the D_{2h}, C_{2v}, and C_{2h} structures. The intensities of the CH stretching region have been reduced by 50×.

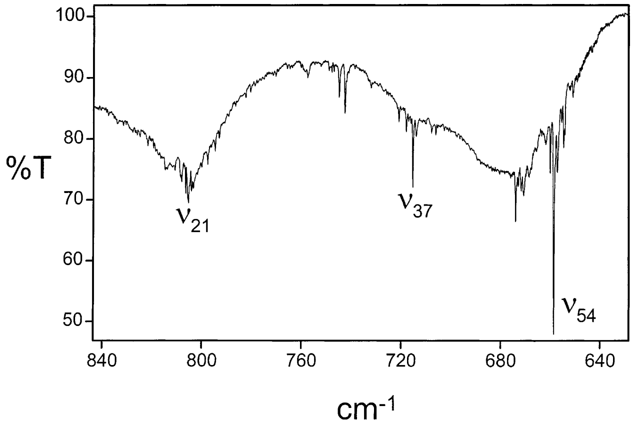

Figure 8. Vapor-phase infrared spectra of BCO in the 640 to 840 cm^{-1} region.

ν_{25}, ν_{26}, and ν_{27} in B_{3g} symmetry (B_2 for C_{2v}). For D_{2h} and C_{2h} symmetry they would be inactive.

Perhaps the strongest evidence for the presence of some molecules existing with C_{2h} symmetry comes from the observed polarized Raman band at 1185 cm^{-1} for ν_{19}. Both D_{2h} and C_{2v} structures would produce only depolarized bands.

It should be mentioned that the ab initio frequency calculation (scaled) does a remarkably good job in predicting the experimental frequencies when using the scaling factors of 0.956 (frequencies above 1800 cm^{-1}) and 0.981 (frequencies below 1800 cm^{-1}). Similar scaling factors have previously been used effectively for 1,2-dihydronaphthalene,[17] tetralin,[18] and 1,4-benzodioxan.[18] The calculations were done for the energy minimum (C_{2v}), trans (C_{2h}), and for the planar structure (D_{2h}) in order to help assign the frequencies to their proper symmetry species. Most of the D_{2h} and C_{2v} frequencies are in close agreement, but ν_8, ν_{21}, and ν_{37} differ significantly, with the C_{2v} values being in much better correspondence with the experimental data. This indicates that for the puckered

TABLE 1: Vibrational Assignments (cm^{-1}) of Bicyclo[3.3.0]oct-1.5-ene

			infrared		Raman				ab initio[a]				
symmetry D_{2h} (C_{2v}, C_{2h})	ν	description[f]	liquid	vapor	liquid		vapor		D_{2h}[c]	C_{2v}[c]		C_{2h}[c]	
A_g (A_1, A_g)	1	β-CH_2 sym. str. (ip′)	(2906)[b]	(2908)[b]	2907 P	(68)	2916	(89)	2921	2917	(29, 88)[e]	2917	(0.90, 84)[e]
	2	α-CH_2 sym. str. (ip, ip′)	(2843)[b]	(2853)[b]	2846 P	(100)	2857	(100)	2873	2858	(52, 100)	2864	(1.5, 100)
IR: ia (C, ia)	3	C = C stretch			1677 P	(42)	1677	(27)	1704	1690	(0, 9.8)	1695	(0, 9.3)
R: P (P, P)	4	α-CH_2 def. (ip, ip′)*			1470 P	(17)	1473	(17)	1486	1480	(0.06, 4.5)	1482	(0, 4.6)
	5	β-CH_2 def. (ip′)*			1441 P	(31)	1446	(24)	1456	1456	(1.8, 7.0)	1456	(0, 7.8)
	6	α-CH_2 wag (ip, op′)	1283 vw		1286 P	(6)	1287	(5)	1295	1292	(0.13, 1.4)	1293	(0, 1.4)
	7	ring stretch		891 mw Q	892 P	(25)	889	(22)	882	885	(0.02, 1.9)	881	(0, 2.4)
	8	ring breathing (ip′)	857 w	856 vw Q	850 P	(12)	852	(14)	811	845	(0.65, 4.8)	834	(0, 4.1)
	9	ring bend (ip, ip′)	536/528 vw	524 w Q	527 P	(13)	522	(7)	530	520	(0.09, 1.6)	519	(0, 1.5)
B_{1g} (A_2, B_g)	10	α-CH_2 sym. str. (op, op′)			(2846)[b]		(2857)[b]		2868	2857	(0, 20)	2861	(0.35, 38)
	11	α-CH_2 def. (op, op′)							1463	1460	(0, 5.7)	1461	(0, 5.9)
IR: ia (ia, ia)	12	α-CH_2 wag (op, ip′)[g]			(1286)[b]	vw			1368	1365	(0, 0.09)	1366	(0, 0.15)
R: D (D, D)	13	β-CH_2 wag (op′)[g]			1328	vw			1262	1287	(0, 0.09)	1286	(0, 0.43)
	14	ring stretch							1162	1146	(0, 1.0)	1146	(0, 0.99)
	15	ring stretch			970 D	(14)	968	vw	956	959	(0, 1.8)	964	(0, 1.8)
	16	skeletal bend (op, op′)	662 vw		665 D	(2)	676	vw	660	654	(0, 0.13)	658	(0, 0.14)
B_{2g} (B_1, A_g)	17	β-CH_2 antisym. str. (op′)	(2948)[b]	(2961)[b]	2952 D	(4)	2954	(42)	2953	2950	(18, 23)	2950	(4.5, 36)
	18	α-CH_2 antisym. str. (ip, op′)	(2894)[b]	(2896)[b]	2896 D	sh			2884	2896	(6.8, 30)	2893	(0.01, 28)
IR: ia (A, ia)	19	α-CH_2 twist (ip, ip′)	1182 vw		1185 P	(5)			1179	1187	(0.56, 2.1)	1183	(0, 2.5)
R: D (D, P)	20	α-CH_2 rock (ip, op′)[g]	996 vw	999 mw Q	- - - - -	- - - - -			968	971	(0.15, 1.1)	972	(0, 1.2)
	21	β-CH_2 rock (op′)[g]	799 vw	805 w Q	801 D	(0.06)			722	797	(0.36, 0.04)	703	(0, 0.55)
	22	ring puckering (op′)							imag	139	(0.07, 0.10)	100	(0, 0.20)
B_{3g} (B_2, B_g)	23	α-CH_2 antisym. str. (op, ip′)					2874	vw	2886	2901	(65, 46)	2896	(1.4, 58)
	24	α-CH_2 twist (op, op′)[g]							1249	1216	(0.77, 0.56)	1227	(0, 0.91)
IR: ia (B, ia)	25	β-CH_2 twist (ip′)[g]	1151 vw	1153 m B	1150 D	(1.5)			1165	1159	(3.1, 0.05)	1165	(0, 0.15)
R: D (D, D)	26	α-CH_2 rock (op, ip′)		901 m B	905 D	(0.7)			922	900	(0.94, 0.23)	906	(0, 0.53)
	27	ring twisting (ip′)	478 mw	485 vw B	478 D	(1)			466	486	(0.28, 0.04)	477	(0, 0.05)
A_u (A_2, A_u)	28	α-CH_2 antisym. str. (op, op′)							2886	2901	(0.03, 8.1)[e]	2896	(47, 1.7)[e]
	29	α-CH_2 twist (op, ip′)[g]							1243	1222	(0, 0.17)	1219	(0.86, 0)
IR: ia (ia, B)	30	β-CH_2 twist (op′)[g]			1102 D	vw			1110	1100	(0, 0.16)	1107	(0.53, 0)
R: ia (ia, ia)	31	α-CH_2 rock (op, op′)							874	866	(0, 0.16)	865	(0.37, 0)
	32	ring twisting (op′)							189	194	(0, 0)	191	(0, 0)
B_{1u} (A_1, B_u)	33	β-CH_2 antisym. str. (ip′)	2948 vvs	2961 vvs Q	2948 P	(37)	(2954)[b]		2953	2950	(49, 19)	2950	(56, 2.9)
	34	α-CH_2 antisym. str. (ip, ip′)	2892 vvs	2896 sh	(2896)[b]				2883	2896	(0.43, 1.2)	2891	(19, 0.02)
IR: C (C, A/C)	35	α-CH_2 twist (ip, op′)	1208 m	1212 vs Q	1208 P	(0.7)			1211	1212	(2.1, 0.14)	1217	(2.5, 0)
R: ia (P, ia)	36	α-CH_2 rock (ip, ip′)	1067 m	1070 vs Q	1070 P	vw			1067	1073	(1.9, 0.11)	1067	(1.6, 0)
	37	β-CH_2 rock (ip′)	718 br	715 w Q	719 P	(0.01)	719	vw	743	714	(0.59, 0.43)	789	(1.1, 0)
	38	ring flapping (ip′)		∼200 br	217 P	vvw			197	229	(4.7, 0.13)	207	(4.2, 0)
	39	ring puckering (ip′)							imag	112	(0.01, 0.11)	74	(0.05, 0)
B_{2u} (B_2, A_u)	40	α-CH_2 sym. str. (op, ip′)	2843 vvs	2857 s B	(2846)[b]		(2858)[b]		2872	2855	(14, 4.9)	2864	(100, 1.4)
	41	α-CH_2 def. (op, ip′)	1461 m	1455 vs B	(1470)[b]		(1473)[b]		1469	1465	(1.7, 0.52)	1466	(1.6, 0)
IR: B (B, B)	42	α-CH_2 wag (op, op′)[g]	1299 m	1308 vw B					1304	1309	(1.1, 0.07)	1305	(1.6, 0)
R: ia (D, ia)	43	β-CH_2 wag (ip′)[g]	1267 m	1275 s B					1250	1273	(5.2, 0.49)	1268	(3.5, 0)
	44	ring stretch	1010 mw	1013 w B	1003 P	(0.07)			1016	1005	(0.43, 0.02)	1008	(0.57, 0)
	45	ring stretch	971 w	974 vw B	(970)[b]	- - - - -	(968)[b]		974	971	(0.08, 0.37)	970	(0.02, 0)
	46	skeletal bend (op, ip′)		365 m B	370 D	(0.2)			360	362	(1.4, 0)	361	(1.1, 0)
B_{3u} (B_1, B_u)	47	β-CH_2 sym. str. (op′)	2906 vvs	2908 m	(2907)[b]		(2916)[b]		2920	2916	(72, 2.2)	2915	(84, 0.83)
	48	α-CH_2 sym. str. (ip, op′)	2843 vvs	2853 m	(2846)[b]		(2857)[b]		2868	2859	(100, 25)	2860	(43, 0.23)
IR: A (A, A/C)	49	β-CH_2 def. (op′)[g]	(1461)[b]	1467 m Q	(1470)[b]		(1473)[b]		1484	1478	(1.8, 0.11)	1480	(1.9, 0)
R: ia (D, ia)	50	α-CH_2 def. (ip, op′)[g]	1448 ms	1446 vs Q	(1441)[b]		(1446)[b]		1456	1455	(0.62, 0.79)	1456	(1.4, 0.01)
	51	α-CH_2 wag (ip, ip′)	1314 vw	1320 w Q	1315 D	vvw			1319	1313	(0.45, 0)	1316	(0.40, 0)
	52	ring stretch	1188 vvw	1193 w Q	(1185)[b]				1166	1162	(0.07, 0.53)	1162	(0.11, 0)
	53	ring breathing (op′)	877 vw	881 vw Q	878 P	(0.4)			872	878	(0.44, 0.06)	877	(0.29, 0)
	54	ring bend (ip, op′)	655 w	659 s Q					712	630	(0.03, 0.01)	658	(0.45, 0)

[a] Calculated using the B3LYP/6-311++G** basis set. [b] () = expected band position obscured by stronger band. [c] Frequency scaled with a scaling factor of 0.981 for frequencies less than 1800 cm^{-1} and 0.956 for frequencies greater than 1800^{-1}. [d] Relative intensities in parentheses. [e] Relative calculated intensities (IR, Raman). [f] Abbreviations: ip, in-phase; op, out-of-phase; ia, inactive; s, strong; m, medium; w, weak; v, very; sh, shoulder; br, broad; P, polarized; D, depolarized. [g] α-CH_2 and β-CH_2 motions are strongly mixed for the rocking, twisting, wagging, and deformation motions.

structure there are vibrational interactions that are not allowed for the highly symmetric D_{2h} form. It might also appear that the frequencies for ν_{21} and ν_{37} are not properly correlated since the frequencies are quite different for the three symmetries. However, they are correct and simply reflect different interactions for the different structures, such as between ν_8 and ν_{37} for C_{2v} and ν_8 and ν_{21} for C_{2h}. As expected, many of the CH_2 vibrations of BCO are very similar in frequency to those of cyclopentene.[3] Not surprisingly the skeletal vibrations differ more in frequency reflecting the interactions between the two rings. The extra strain in BCO also pushes the C═C stretching up to 1677 cm^{-1} as compared to 1617 cm^{-1} in cyclopentene.

It should be noted that the vibrational spectra predicted for the D_{2h}, C_{2h}, and C_{2v} (energy minimum) conformations are only somewhat different, with the principal features remaining the same. Figures 6 and 7 compare the calculated infrared and Raman spectra, respectively, for the three structures and these can be seen to be similar. However, closer comparison to the experimental data (Table 1 and Figures 3 − 5) clearly shows the best agreement with the C_{2v} calculations.

Attempts are still underway to record the far-infrared spectra of BCO, but its low vapor pressure and low dipole moment have so far not allowed the ring-puckering spectra to be recorded. There does appear to be evidence for puckering combination bands in the 640 to 840 cm^{-1} region of the infrared spectrum, and these are shown in Figure 8. Although three of the bands have been assigned to fundamentals, this region is rich with other bands that are likely combinations of the ν_{39} puckering motion with A_g fundamentals ν_9 (532 cm^{-1}), ν_8 (852 cm^{-1}), or ν_7 (889 cm^{-1}). The many bands near 800 cm^{-1} may all be due to combinations rather than ν_{21}. The following paper will present a theoretical discussion of the expected puckering spectra, and further experimental work is also in progress.

Conclusion

Ab initio calculations indicate that BCO is a mixture of C_{2v} and C_{2h} puckered forms, with the latter about 229 cm^{-1} higher in energy (65 cm^{-1} in the unflapped form). The planar form is calculated to be 408 cm^{-1} higher in energy for the unflapped form. The structure for the actual energy minimum also shows a small amount of flapping which is calculated to stabilize the molecule by an additional 164 cm^{-1} (0.40 kcal/mol), raising the barrier to planarity to 572 cm^{-1}. The vibrational spectra can be assigned quite well on the basis of D_{2h} (planar) symmetry, but additional bands, particularly for B_{1u} and B_{3g} vibrations, clearly demonstrate that the two rings are puckered with the C_{2v} structure dominating. These results are consistent with the previous electron diffraction study. However, the high level ab initio calculations provide a considerably clearer picture of the energy differences between the two energy minima, and the spectra show the C_{2v} form to be dominant. The ab initio calculation predicts dihedral angles of puckering of 26°, which is the same as the value found for cyclopentene.

Acknowledgment. The authors thank the National Science Foundation and the Robert A. Welch Foundation for financial assistance.

References and Notes

(1) Laane, J.; Lord, R. C. *J. Chem. Phys.* **1967**, *47*, 4941.
(2) Chao, T. H.; Laane, J. *Chem. Phys Lett.* **1972**, *14*, 595.
(3) Villarreal, J. R.; Laane, J.; Bush, S. F.; Harris, W. C. *Spectrochim. Acta*, **1979**, *35A*, 331.
(4) Villarreal, J. R.; Bauman, L. E.; Laane, J.; Harris, W. C.; Bush, S. F. *J. Chem. Phys.* **1975**, *63*, 3727.
(5) Villarreal, J. R.; Bauman, L. E.; Laane, J. *J. Phys. Chem.* **1976**, *80*, 1172.
(6) Bauman, L. E.; Killough, P. M.; Cooke, J. M.; Villarreal, J. R.; Laane, J. *J. Phys. Chem.* **1982**, *86*, 2000.
(7) Laane, J. *Pure Appl. Chem.* **1987**, *59*, 1307.
(8) Laane, J. In *Structures and Conformations of Non-Rigid Molecules*, J. Laane, M. Dakkouri, B. van der Veken, and H. Oberhammer, Eds.; Amersterdam, 1993; Chapter 4.
(9) Laane, J. *Annu. Rev. Phys. Chem.* **1994**, *45*, 179.
(10) Laane, J. *Int. Rev. Phys. Chem.* **1999**, *18*, 301.
(11) Laane, J. *J. Phys. Chem. A* **2000**, *33*, 7715.
(12) Mastryukov, V. S.; Arkhipova, E. Y.; Traetteberg, M.; Almenningen, A. *Acta Chem. Scand*. **1989**, *43*, 238.
(13) Arkhipova, E. Y.; Mastryukov, V. S.; Traetteberg, M. *J. Mol. Struct*. **1990**, *216*, 333.
(14) Kopecky, K. R.; Lockwood, P. A.; Gomez, R. R.; Ding, J.-Y. *Can. J. Chem.* **1981**, *59*, 851.
(15) Haller, K.; Chiang, W.-Y.; del Rosario, A.; Laane J. *J. Mol. Struct*. **1996**, *379*, 19.
(16) Autrey, D.; Choo, J.; Laane, J. *J. Phys. Chem. A* **2001**, *105*, 10230.
(17) Autrey, D.; Arp, Z.; Choo, J.; Laane, J. *J. Chem. Phys.* **2003**, *115*, 2557.
(18) Autrey, D.; Yang, J.; Laane, J. *J. Mol. Struct.*, in press.